were particularly rapid, **4** was added as a solid to the cell containing CH_2Cl_2 (3.0 mL) at 20 °C. The solid, which was finely divided, rapidly dissolved.

The initial concentration of **4** was obtained by comparison of the optical density of the equilibrium mixture with that of a reference solution. When other reactants were present, the initial concentration was obtained by using the program and extrapolation back to zero time.

Since **4b** and **4c** react in CH_2Cl_2 even in the absence of added acid or base, molar extinction coefficients were obtained by extrapolation of the optical densities at 280 nm to zero time. The following values were obtained: ϵ_{4b} 10 500 ± 100; ϵ_{4c} = 10 450 ± 50. Since **4a** does not react in neutral CH_2Cl_2 the following value was measured directly: ϵ_{4a} 10 700.

At 280 nm dicyclohexylcarbodiimide (**2**) and the thiophosphate anion **3′** do not have a significant absorption so that the optical density at equilibrium can be determined from eq 5, derived from eq 4.

$$\underset{x_0 - x}{4} \rightleftharpoons \underset{y}{2} + \underset{y}{3'} + \underset{x-y}{5'} \tag{4}$$

$$OD_{equil} = (x_0 - x)\epsilon_4 + (x - y)\epsilon_3 \tag{5}$$

The molar extinction coefficient for **5** cannot be obtained directly, but it is safe to assume that because of the relative acidity of **3** and the basicity of **5** that the concentration of free **5** present in solution will be negligible. Since it was confirmed (by IR and ^{31}P NMR) that **2** = **5′** = **3′**, eq 5 reduces to eq 6, and thus the concentration of **4** at equilibrium is given by eq 7.

$$OD_{equil} = (x_0 - x)\epsilon_4 + (x/2)\epsilon_3 \tag{6}$$

$$x_e = x_0\left[1 - \frac{\frac{OD_{equil}}{x_0} - \epsilon_4}{\frac{\epsilon_3}{2} - \epsilon_4}\right] \tag{7}$$

When **4** is treated with base its concentration varies with time according to eq 2 which is derived from eq 8. The initial value of $[4]_0$ is

$$4 \underset{k_{-1}}{\overset{k_1}{\rightleftharpoons}} 5 \xrightarrow{k_2} \text{products} \tag{8}$$

known as is k_1 and the other constants given in eq 9–11.

$$r_1 = \frac{-(k_1 + k_{-1} + k_2) + \{[(k_1 + k_{-1}) - k_2]^2 + 4k_{-1}k_2\}^{1/2}}{2} \tag{9}$$

$$r_2 = \frac{-(k_1 + k_{-1} + k_2) - \{[(k_1 + k_{-1}) - k_2]^2 + 4k_{-1}k_2\}^{1/2}}{2} \tag{10}$$

$$P_1 = \frac{[4]_0(r_2 - k_1)}{r_1 - r_2};\ Q_1 = \frac{[4]_0(r_1 - k_1)}{r_2 - r_1} \tag{11}$$

The other constants were determined by using a computer program with a least-squares minimization routine. An example of the resultant optical density vs. time plots (experimental and calculated are given in Figure 4).

In the presence of excess base, **3** is converted to the counterion **3′** so that the formation of **2** and **3′** is essentially irreversible. Under these conditions **5** does not accumulate in solution (tight isosbestic points are held), and the steady-state approximation for the concentration of **5** can be applied. This leads to eq 12, and using the values of k_1, k_{-1}, and k_2

$$k_{obsd} = \frac{k_1 k_2}{k_2 + k_{-1}} \tag{12}$$

already determined reproduces closely the observed rate constants (see Table VII).

Registry No. **3a**, 2253-60-3; **3b**, 7355-10-4; **3c**, 81640-00-8; **3′a**, 55979-88-9; **3′b**, 83599-87-5; **3′c**, 92366-09-1; **4a**, 92366-10-4; **4b**, 83599-89-7; **4c**, 92366-11-5; **5′a**, 92366-13-7; **5′b**, 85329-00-6; **5′c**, 92366-15-9; $EtNCH_2CH_2OCH_2CH_2$, 100-74-3; Et_3N, 121-44-8; 1,8-bis(dimethylamino)naphthalene, 20734-58-1; dicyclohexylcarbodiimide, 538-75-0.

Nondissociative Permutational Isomerization of an Octahedral Derivative of a Nonmetallic Element, a 12-Te-6 Species[1]

Ronald S. Michalak, Scott R. Wilson, and J. C. Martin*

Contribution from the Roger Adams Laboratory, University of Illinois, 1209 West California St., Urbana, Illinois 61801. *Received April 16, 1984. Revised Manuscript Received August 4, 1984*

Abstract: The reactions of bromine trifluoride with 3,3,3′,3′-tetramethyl-1,1′-spirobi[3*H*-2,1-benzoxatellurole] (**9**) and 6,6′-bis(1,1-dimethylethyl)-3,3,3′,3′-tetrakis(trifluoromethyl)-1,1′-spirobi[3*H*-2,1-benzoxatellurole] (**10**) give rise to the *all-trans*-12-Te-6 species, pertelluranes **3** [1,1-difluoro-1,1-dihydro-3,3,3′,3′-tetramethyl-1,1′-spirobi[3*H*-2,1-benzoxatellurole]-(*OC*-6-12)], and **13** [6,6′-bis(1,1-dimethylethyl)-1,1-difluoro-3,3,3′,3′-tetrakis(trifluoromethyl)-1,1′-spirobi[3*H*-2,1-benzoxatellurole]-(*OC*-6-12)]. Pertelluranes **3** and **13** have two trans fluorines, two trans oxygens, and two trans carbons at ligation sites about the central tellurium atom. The rate of isomerization from the all-trans geometry of **3** to (*OC*-6-22) stereoisomer **4**, with cis fluorines and oxygens and trans carbons, was determined in different solvents and at different concentrations at 61 °C. Failure to trap fluoride ion by added hexadimethyldisilazane provides evidence against a dissociative mechanism involving Te–F bond heterolysis to give dissociation ions. The similarity of first-order rates of reaction [2.0×10^{-5} to 2.5×10^{-5} s^{-1} at 61 °C] in solvents of differing ionizing power (Y values in the range −5.57 to −8.62, m = 0.03) provides evidence ruling out heterolytic dissociation mechanisms for the isomerization of **3** to **4**, including those with ion pair or zwitterionic intermediates. The mechanism for the permutational isomerization is concluded to be a nondissociative twist involving cleavage of none of the six bonds to tellurium. The lower activation barrier for the trigonal twist of 12-Te-6 pertellurane **3** ($\Delta G^*_{61°C}$ = 27 kcal/mol) compared to *all-trans*-12-S-6 persulfane **1** (not observed, $\Delta G^* > 50$ kcal/mol) and the relative energies of the observed stereoisomers of **1** and **3** are discussed in terms of observed ground-state trigonal distortion. The isomerization of **13** to a stereoisomer was not observed, either thermally or in the presence of Lewis acids. This could result from a higher activation barrier for the isomerization or **13** could represent the most thermodynamically stable isomer in the set of possible stereoisomers. The results of complete X-ray crystallographic structure determinations of pertellurane **4** and tellurane **5** are described.

Mechanisms of the often facile ligand rearrangements of trigonal-bipyramidal (TBP) 10-X-5[1] (X = P[2a,b], Si,[2c-g] As,[2h] Sb[2h]) compounds have been a subject of continuing ineterest, especially for 10-P-5 phosphoranes. Ligand rearrangements of 10-X-4 (X

0002-7863/84/1506-7529$01.50/0

= S^{3a-c}, $Se^{3d,e}$, Te^{3e}) pseudo-trigonal-bipyramidal (ψ-TBP) species have been studied to a lesser extent. Many possible mechanisms for the permutation of substituents in TBP species have been thoroughly discussed.[4-6]

Although analogous permutational isomerization mechanisms for octahedral (*OC*) nonmetallic elements have received relatively little attention, mechanistic investigations have been carried out on a large number of *OC* metal complexes.[7] Dissociative and nondissociative mechanisms have been described for ligand rearrangements of these complexes.

Evidence[7] for intramolecular rearrangement of *OC* species has most often come from dynamic NMR determinations of site-exchange processes for ligands occupying nonequivalent sites. Sometimes the retention of spin–spin coupling can provide[8] powerful evidence for the intramolecular nature of rearrangements of appropriately designed molecules. A probable mechanism for the exchange can sometime be deduced[7a,b] from the detailed information dynamic NMR can provide. Heavy use of Occam's razor to excise more complex reaction mechanisms from the set of schemes being considered has often led to the postulation of a trigonal twist mechanism for intramolecular rearrangements. In this commonly postulated mechanism two *OC* species are interconverted through a transition state with the geometry of the trigonal prism (*TP*). In a few cases bicapped tetrahedral geometries have been postulated[8a] to play important roles in rearrangements of transition metals with hydride ligands.

Detailed nondissociative pathways have been described for attaining a transition state with local *TP* geometry from an *OC* ground state. The reaction coordinate can be one which maintains either local C_3 symmetry (Bailar twist[9]) or C_2 symmetry (Ray–Dutt[10] or Springers–Sievers twist[11]) at the reaction center. Such distinctions are more meaningful in symmetrically substituted *OC* species with three bidentate ligands. If one considers only local symmetry (the bonds to the central atom, without regard to the identity of the substituent) then the small differences in geometry encountered along these two pathways can be ignored. This is particularly true in cases in which unsymmetrical substitution induces distortion from ideal *OC* geometry in the ground state and ideal *TP* geometry in the transition state. We will follow precedent[12] in discussing the twist mechanism which we postulate for an *OC* 12-Te-6 species in terms of the trigonal twist.

In many cases for which trigonal twists have been postulated, alternative, somewhat more complex mechanisms, involving single bond scission, have not been ruled out. Single bond heterolysis to give an ion pair, for example, provides a pathway for a cleanly intramolecularly rearrangement if ion pair return to give rearranged product is rapid compared to dissociation. The cleavage of a single bond at one site of a bidentate ligand will not be followed by dissociation unless a second bond is broken. This mechanism was recognized as a possibility for the intramolecular isomerization of *OC* complexes by Werner[13] in 1912. The *TBP* 10-X-5 species which is formed by heterolysis of one bond of an *OC* species could in many cases be expected to undergo facile ligand permutation before reforming the bond to generate an isomeric *OC* species.

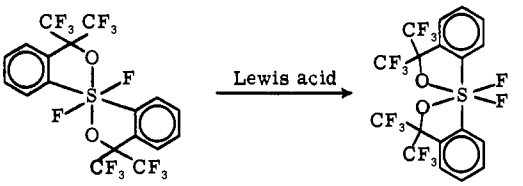

1 **2**

The operation of a dissociative, acid-catalyzed mechanism has been established[15] for the isomerization of (*OC*-6-12)[16]-*trans*-persulfurane **1** to (*OC*-6-22)-*cis*-**2**. Even at high temperatures no evidence was obtained, in the absence of acid catalysts, for a nondissociative, intramolecular isomerization of **1** to **2**. This sets a lower limit of 50 kcal/mol for the activation barrier for this process. Nondissociative isomerizations of some 12-P-6 phosphorus anions have recently been proposed,[17a,b] but possible mechanisms involving the cleavage of endocyclic P–X bonds were not unambiguously ruled out.[17c]

We here report evidence, from studies of the dependence or rate on solvent ionizing power, for an intramolecular, nondissociative isomerization of the *all-trans*-(*OC*-6-12)-pertellurane **3** to *cis*-(*OC*-6-22)-pertellurane **4**. An X-ray crystallographic structure determination of the 12-Te-6 species, **4**, has also been completed. The X-ray crystallographic structure determination reported here for a 10-Te-4 species, tellurane **5**, is one of a series of structures of isoelectronic and isostructural nonmetallic species which have been reported, including those of sulfurane **6**[18] (10-S-4) and periodonium cation **7**[19] (10-I-4). Phosphoranide anion **8**

(1) Compounds in this paper are designated by the *N*-X-*L* formalism where *N* is the number of valence-shell electrons about atom X which are formally involved in bonding *L* ligands to X. See: Perkins, C. W.; Martin, J. C.; Arduengo, A. J.; Lau, W.; Alegria, A.; Kochi, J. K. *J. Am. Chem. Soc.* **1980**, *102*, 7753.

(2) (a) Holmes, R. R. "Pentacoordinated Phosphorus. Structure and Spectroscopy"; American Chemical Society: Washington, DC, 1980, Vol. I and II. (b) Luckenbach, R. "Dynamic Stereochemistry of Pentacoordinated Phosphorus and Related Elements"; Georg Theime Verlag: Stuttgart, 1973. (c) Farnham, W. B.; Harlow, R. L. *J. Am. Chem. Soc.* **1981**, *103*, 4608. (d) Corriu, R. J. P.; Guerin, C. *J. Organomet. Chem.* **1980**, *198*, 231. (e) Stevenson, W. H., III; Martin, J. C. *J. Am. Chem. Soc.* **1982**, *104*, 309. (f) Stevenson, W. H., III; Martin, J. C. *Phosphorus Sulfur*, **1983**, *18*, 81. (g) Stevenson, W. H., III; Martin, J. C. *J. Am. Chem. Soc.*, submitted for publication. (h) Holmes, R. R. *Acc. Chem. Res.* **1979** *12*, 257.

(3) (a) Astrologes, G. W.; Martin, J. C. *J. Am. Chem. Soc.* **1976**, *98*, 2895. (b) Klemperer, W. G.; Krieger, J. K.; McCreary, M. D.; Muetterties, E. L.; Traficante, D. D.; Whitesides, G. M. Ibid. **1975**, *97*, 7023. (c) Belkind, B. A.; Denney, D. B.; Denney, D. Z.; Hsu, Y. F.; Wilson, G. E., Jr. *Ibid.* **1978**, *100*, 6327. (d) Reich, H. *Ibid.* **1973**, *95*, 964. (e) Denney, D. B.; Denney, D. Z.; Hammond, P. J.; Hsu, Y. F. *Ibid.* **1981**, *103*, 2340.

(4) Berry, R. S. *J. Chem. Phys.* **1960**, *32*, 933.

(5) Ugi, I.; Marquarding, D.; Klusacek, H.; Gillespie, P.; Ramirez, F. *Acc. Chem. Res.* **1971**, *4*, 288 and references cited therein.

(6) (a) Muetterties, E. L. *J. Am. Chem. Soc.* **1969**, *91*, 1636. (b) Muetterties, E. L. *Ibid.* **1969**, *91*, 4115. (c) Musher, J. I.; Cowley, A. H. *Inorg. Chem.* **1975**, *14*, 2302.

(7) (a) Pignolet, L. H. *Top. Curr. Chem.* **1975**, *56*, 91. (b) Serpone, N.; Bickley, D. G. *Prog. Inorg. Chem.* **1972**, *17*, 391. (c) Fortman, J. J.; Sievers, R. E. *Coord. Chem. Rev.* **1971**, *6*, 331. (d) Muetterties, E. L. *J. Am. Chem. Soc.* **1968**, *90*, 5097.

(8) For example, see: (a) Meakin, P.; Muetterties, E. L.; Jesson, J. P. *J. Am. Chem. Soc.* **1973**, *95*, 75. (b) Pomeroy, R. K.; Vancea, L.; Calhoun, H. P.; Graham, W. A. G. *Inorg. Chem.* **1977**, *16*, 1508. (c) Vancea, L.; Bennett, M. J.; Jones, C. E.; Smith, R. A.; Graham, W. A. G. *Ibid.* **1977**, *16*, 897. (d) Vancea, L.; Graham, W. A. G. *J. Organomet. Chem.* **1977**, *134*, 219.

(9) Bailar, J. C., Jr. *J. Inorg. Nucl. Chem.* **1958**, *8*, 165.

(10) Ray, P.; Dutt, N. K. *J. Indian Chem. Soc.* **1943**, *20*, 81.

(11) Springer, C. S., Jr.; Sievers, R. E. *Inorg. Chem.* **1967**, *6*, 852.

(12) Hoffman, R.; Howell, J. M.; Rossi, A. R. *J. Am. Chem. Soc.* **1976**, *98*, 2484.

(13) Werner, A. *Ber.* **1912**, *45*, 3061.

(14) One possible way to rule out such a mechanism uses a correlation between mechanisms of isomerization and volumes of activation. Lawrance, G. A.; Stranks, D. R. *Acc. Chem. Res.* **1979**, *12*, 403.

(15) Michalak, R. S.; Martin, J. C. *J. Am. Chem. Soc.* **1982**, *104*, 1683.

(16) We use the (*OC*-6-*XY*) system to define the stereochemistry of octahedral compounds. The symmetry code *OC* designates octahedral geometry and 6 refers to the number of substituents about the central atom. The first digit, *X*, of the two-digit configuration number is the Cahn–Ingold–Prelog, CIP, priority number of the substituent trans to the most preferred substituent of priority 1. (When two substituents have the same priority number of 1, the preferred substituent is that opposite the substituent having the larger CIP priority number.) These two atoms define the principal axis of the octahedron. The second digit, *Y*, of the configuration number is the CIP priority number for the substituent trans to the most preferred ligating atom (lowest CIP priority number) in the plane perpendicular to the principal axis. For further details see: Brown, M. F.; Cook, B. R.; Sloan, T. E. *Inorg. Chem.* **1975**, *14*, 1273. The chirality symbols Δ and Λ are assigned according to IUPAC rule 7.8. See IUPAC Rule 7.8, *Pure Appl. Chem.* **1971**, *28*, 75.

(17) (a) Font Freide, J. J. H. M.; Trippett, S. *J. Chem. Soc., Chem. Commun.* **1980**, 934. (b) Font Freide, J. J. H. M..; Trippett, S. *J. Chem. Res. Synop.* **1981**, 218. (c) Reference 17a and 17b report evidence that the permutational isomerization about 12-P-6 phosphorus is intramolecular. Since the hexacoordinate phosphate anion has two bidentate ligands to phosphorus, however, an alternative to the nondissociative (twist) mechanism must be considered, namely dissociative cleavage at one ligation site of a bidentate ligand.[15] Evidence for a parallel sort of intramolecular dissociative mechanism involving endocyclic bond heterolysis has been described[3e] for a ψ-TBP 10-Se-4 species.

(18) Perozzi, E. F.; Martin, J. C.; Paul, I. C. *J. Am. Chem. Soc.* **1974**, *96*, 6735.

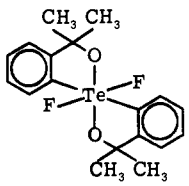

3

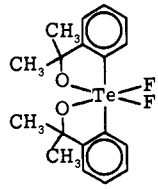

4

(10-P-4), isoelectronic with **5**, **6**, and **7**, has also been isolated and characterized.[20] The X-ray crystallographic structures of some 12-Te-5 pertelluranes have recently been reported.[21]

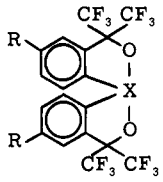

5 X = Te, R = H
6 X = S, R = t-butyl
7 X = I^+, R = H
8 X = P^-, R = H

Experimental Section

General Procedures. Chemical shifts for ^1H, ^{19}F, and ^{125}Te NMR are reported on the δ scale, ppm downfield from the internal standards Me_4Si, $CFCl_3$, and Me_2Te, respectively. Experimental techniques for ^{125}Te NMR have previously been discussed.[3e,22] Teflon apparatus was dried at 140 °C for several hours before use. Elemental analyses are within 0.4% of values calculated for the listed elements, unless otherwise indicated.

Caution! Bromine trifluoride is a very powerful oxidizing agent which should be used with care. All operations involving BrF_3 were conducted under N_2 in dry Teflon apparatus with $CF_2ClCFCl_2$, dried by distillation from P_2O_5, as solvent.

3,3,3′,3′-Tetrakis(trifluoromethyl)-1,1′-spirobi[3*H*-2,1-benzoxatellurole] (5). Methylmagnesium bromide (20 mL, 31.1 M in ether, 63 mmol) was added dropwise at 0 °C with magnetic stirring to 1,1,1,3,3,3-hexafluoro-2-(2-iodophenyl)-2-propanol (23 g, 62 mmol) in 150 mL of dry tetrahydrofuran (THF). Magnesium metal (1.5 g, 0.062 g-atom, 70–80 mesh) was added, and the mixture was boiled for 5 h. Tellurium tetrachloride (8.5 g, 31 mmol) in 50 mL of dry THF was added dropwise at 0 °C. This mixture was boiled for 30 min, cooled, and filtered. Removal of solvent and recrystallization from ether gave 3.5 g (5.7 mmol, 20%) of **5**: mp 211–212 °C; ^1H NMR ($CDCl_3$) δ 7.8–8.1 (m, 6, Ar *H*), 8.3-8.5 (M, 2, Ar *H* ortho to Te); ^{19}F NMR ($CDCl_3$) δ −74.0 and −76.8 (A_3B_3 pattern, J = 11.2 Hz); ^{125}Te NMR (C_6H_6) δ 1196 (s): mass spectrum (70 eV), m/e (relative intensity) 595 (4, $M^{+\cdot} - F$), 545 (100, $M^{+\cdot} - CF_3$). Anal. ($C_{18}H_8F_{12}O_2Te$): C, H, Te.

3,3,3′,3′-Tetramethyl-1,1′-spirobi[3*H*-2,1-benzoxatellurole] (9). Methylmagnesium bromide (8 mL, 3.1 M in ether, 25 mmol) was added dropwise at 0 °C with magnetic stirring to 2-(2-bromophenyl)propanol (4.8 g, 22.3 mmol) and 50 mL of dry THF. Magnesium powder (0.54 g, 22.5 mg-atom, 70–80 mesh) was added and the solution boiled overnight. Tellurium tetrachloride (3.0 g, 11.1 mmol) in 30 mL of dry THF was added dropwise to the solution at 0 °C. This mixture was boiled for 1 h and filtered, and solvent was removed. The resulting oil was dissolved in CH_2Cl_2, washed with 200 mL of water, and dried ($MgSO_4$). Recrystallization (CH_2Cl_2) gave 2.7 g (6.8 mmol, 61%) of **9**: mp 207–210 °C; ^1H NMR ($CDCl_3$) δ 7.2–7.3 (m, 2, Ar *H*), 7.4–7.5 (m, 4, Ar *H*), 8.0–8.1 (m, 2, Ar *H*), 1.53 (s, 6, CH_3) 1.58 (s, 6, CH_3); ^{125}Te NMR ($CDCl_3$) δ 1051 (s); mass spectrum (10 eV), m/e (relative intensity) 383 (100, $M^{+\cdot} - CH_3$). Anal. ($C_{18}H_{20}O_2Te$): C, H, Te.

6,6′-Bis(1,1-dimethylethyl)-3,3,3′,3′-tetrakis(trifluoromethyl)-1,1′-spirobi[3*H*-2,1-benzoxatellurole] (10). A solution of *sec*-butyllithium (55 mL of a 1.4 M cyclohexane solution, 77 mmol) in 50 mL of dry ether and 25 μL (0.7 mmol) of *N,N,N′,N′*-tetramethylethylenediamine (TMEDA) was stirred at −80 °C while another solution of 10 g of 1,1,1,3,3,3-hexafluoro-2-(4-*tert*-butylphenyl)-2-propanol (33 mmol) in 100 mL of dry ether was added dropwise. The suspension was warmed slowly to 25 °C. It was then cooled to −80 °C and 5.0 g of $TeCl_4$ (19 mmol) in 50 mL of dry THF was added dropwise. Then the reaction was quenched with methanol and filtered, and solvent was removed. The crude product was chromatographed on silica gel with CH_2Cl_2 as an eluant. The first fraction gave 4.42 g of **10** (6.1 mmol, 37%) as a white solid after recrystallization from CH_2Cl_2/pentane: mp 193–195 °C; ^1H NMR ($CDCl_3$) δ 8.10–8.12 (m, 2, TeCC*H*), 7.60–7.65 (m, 4, Ar *H*), 1.33 (s, 18, CH_3); ^{19}F NMR ($CDCl_3$) δ −72.7, −75.6 (A_3 B_3, J = 11 Hz); ^{125}Te NMR ($CDCl_3$) δ 1190 (s); mass spectrum (10 eV), m/e (relative intensity) 726 (1, $M^{+\cdot}$), 711 (4, $M^{+\cdot} - CH_3$), 657 (100, $M^{+\cdot} - CF_3$). Anal. ($C_{26}H_{24}F_{12}O_2Te$): C, H, Te.

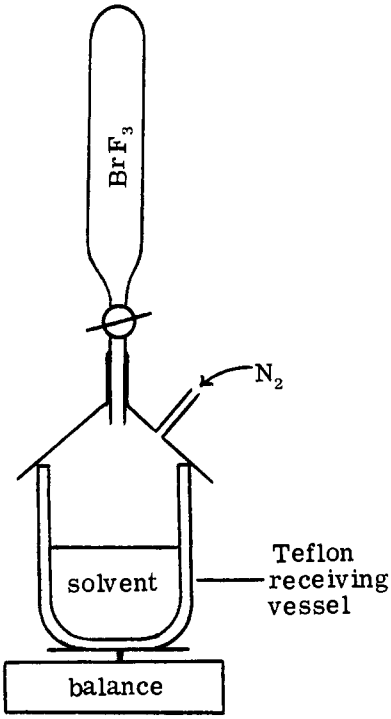

Figure 1. Apparatus for the transfer of bromine trifluoride.

Attempted Oxidation of 5 with Ozone. Ozone was bubbled through a solution of **5** (20 mg, 0.03 mmol) in CH_2Cl_2 at −80 °C until the solution was a blue color. It was then warmed to room temperature. The ^{19}F NMR spectrum showed only unaltered starting material.

Reaction of Tellurane 9 with Ozone To Give 12. Ozone was bubbled through a solution of **9** (20 mg, 0.05 mmol) in CH_2Cl_2 at −80 °C until the solution became blue. It was then warmed to room temperature. Evaporation of solvent gave 15 mg (3.6 mmol, 71%) of slightly impure **12**. Thin-layer chromatography with 50% CH_2Cl_2/hexane on basic alumina showed a single spot, R_F = 0.66: mp 272–275 °C dec; ^1H NMR ($CDCl_3$, 360 MHz) δ 1.40 (s, 12, CH_3), 1.71 (s, 12, CH_3), 6.6–6.8, 7.1–7.4 (m 16, Ar *H*); mass spectrum (10 eV), m/e (relative intensity 828 (4%, $M^{+\cdot}$), 813 (100, $M^{+\cdot} - CH_3$), 798 (5, $M^{+\cdot} - 2\ CH_3$), 414 (71, $M^{+\cdot}$ of monomer), 399 (99, $M^{+\cdot} - CH_3$ of monomer); osmometric M (CH_2Cl_2) 820.

1,1-Difluoro-1,1-dihydro-3,3,3′,3′-tetramethyl-1,1′-spirobi[3*H*-2,1-benzooxatellurole]-(*OC*-6-12) (3). The apparatus shown in Figure 1 was used to make up a solution of BrF_3 (0.12 g, 0.88 mmol) in 20 mL of $CF_2ClCFCl_2$ under a nitrogen atmosphere. The inverted funnel and BrF_3 cylinder were then replaced by a cap for the receiving vessel which provided a mechanism for transfer of the BrF_3 solution via Teflon tubing, using nitrogen pressure, to a second Teflon vessel containing 0.50 g (1.3 mmol) of tellurane **9** and 100 mL of $CF_2ClCFCl_2$ at −20 °C under a nitrogen atmosphere. Removal of solvent and recrystallization from methylene chloride gave 0.17 g (0.39 mmol, 30%) of **3**: mp 220–223 °C; ^1H NMR ($CDCl_3$) δ 8.18 (d, J_{H-H} = 7.5 Hz, 2, Ar *H* ortho to Te), δ 7.50–7.67 (m, 6, Ar *H*), 1.71 (s, 12, CH_3); ^{19}F NMR ($CDCl_3$) δ −25.9 (s, CF_3); ^{125}Te NMR ($CDCl_3$) δ 985 (t, J_{Te-F} = 2108 Hz); mass spectrum (70 eV), m/e (relative intensity) 436 (3, $M^{+\cdot}$), 421 (100, $M^{+\cdot} - CH_3$), 417 (75, $M^{+\cdot} - F$). Anal. ($C_{18}H_{20}F_2O_2Te$): C, H.

6,6′-Bis(1,1-dimethylethyl)-1,1-difluoro-3,3′,3′,3′-tetrakis(trifluoromethyl)-1,1′-spirobi[3*H*-2,1-benzoxatellurole]-(*OC*-6-12) (13). Tellurane **10** (1.0 g, 1.3 mmol) was treated with BrF_3 (0.18 g, 1.3 mmol) according to the procedure discussed for the preparation of **3**. Solvent removal and recrystallization from CH_2Cl_2/hexane gave 0.75 g of **13** (0.98 mmol, 75%): mp 190–192 °C; ^1H NMR ($CDCl_3$) δ 1.46 (s, 18, CH_3), 7.92 (br s, 4, Ar *H*), 8.24 (br s, 2, Ar *H* ortho to Te); ^{19}F NMR ($CDCl_3$) δ −63.4 (s, 2, Te*F*), −75.7 (s, 12, CF_3); ^{125}Te NMR ($CDCl_3$) δ 1007 (t, J_{Te-F} = 2815 Hz); mass spectrum (70 eV), m/e (relative intensity) 764 (2, $M^{+\cdot}$), 749 (29, $M^{+\cdot} - CH_3$), 745 (22, $M^{+\cdot} - F$), 707 (5, $M^{+\cdot}$ – *tert*-butyl), 695

(19) (a) Dess, D. B.; Martin, J. C. *J. Am. Chem. Soc.* **1982**, *104*, 902. (b) Dess, D. B.; Martin, J. C., manuscript in preparation.
(20) Granoth, I.; Martin, J. C. *J. Am. Chem. Soc.* **1979**, *101*, 4623.
(21) Detty, M. R.; Luss, H. R. *J. Org. Chem.* **1983**, *48*, 5149.
(22) (a) Harris, R. K.; Mann, B. E. "NMR and the Periodic Table"; Academic Press: New York, 1978; Chapter 12. (b) Brevard, C.; Granger, P. "Handbook of NMR"; John Wiley and Sons: New York, 1981; p 172.

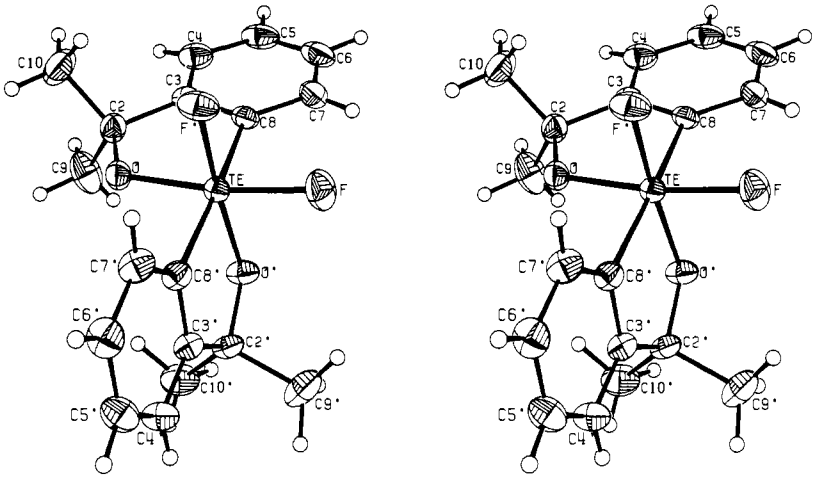

Figure 2. Stereoscopic view of a single molecule of isomer **4**.

(66, $M^{+\cdot} - CF_3$). Anal. Calcd for $C_{26}H_{24}F_{14}O_2Te$: C, H, F.

Isomerization of *trans*-3 to *cis*-4. A. Sulfur trioxide (0.030 g of a 3.2 wt % solution in chloroform-*d*, 1.2×10^{-5} mol) was added to a solution of *trans*-**3** (5 mg, 10^{-5} mol) in 0.4 mL of dry $CDCl_3$. After 1 day and 2 day ^{19}F NMR spectra showed 92 ± 3% of *cis*-**4** and 8 ± 3% of *trans*-**4** ($\Delta G_{25°C}$, 1.4 ± 0.2 kcal/mol). Recrystallization from CH_2Cl_2/hexane gave 4 mg (8×10^{-6} mol, 80%) of **4**: mp 234–235 °C; ^1H NMR ($CDCl_3$) δ 1.55 (s, 6, CH_3), 1.62 (s, 6, CH_3), 7.50–7.70 (m, 6, Ar *H*), 8.13–8.17 (m, 2, Ar *H* ortho to Te; ^{19}F NMR ($CDCl_3$) δ −51.6 (s, Te*F*); ^{125}Te NMR ($CDCl_3$) δ 1066 (t, J_{Te-F} = 2629 Hz); Anal. Calcd for $C_{18}H_{20}F_2O_2Te$: C, H.

B. A solution of 8.7 mg (2.0×10^{-5} mol) of *trans*-**3**, 0.4 mL of quinoline, and 0.4 mL of 1,2-dichloroethane was heated to 60 °C for 60 h. The ^{19}F NMR spectrum showed the disappearance of *trans*-**3** and the appearance of *cis*-**4**. The ratio of cis and trans isomers was approximately 9:1.

Reaction of 3 with Diphenyl Ether. A solution of *trans*-**3** (0.45 g, 1.03 mmol) in 5 mL of diphenyl ether, after 10 h at 97 °C, gave 0.35 g, 0.81 mmol (79%) of tellurane **5**, which was identified by its mass spectrum, elemental analysis, and melting point. The ^{19}F NMR spectrum of the solution showed a broad peak at δ −127, the region for aryl fluorides. The fluorine-containing products were not isolated.

Attempted Isomerizations of 13. A. The ^{19}F NMR spectrum of a solution of **13** (21.6 mg, 0.030 mmol) and SbF_5 (3 mg, 0.01 mmol) in 0.4 mL of $CHCl_3$ showed no detectable isomerization (<3%) after being boiled for 3 days.

B. Pertellurane **13** (100 mg, 0.131 mmol) was heated in a Teflon vessel at 210 °C for 96 h at 0.4 torr. The ^{19}F NMR spectrum showed no detectable isomerization (<3%). This sets a lower limit of 44 kcal/mol for the activation barrier for the thermal isomerization of **13**.

Kinetic Measurements: Thermal Isomerization of 3. The solutions used to measure the rate of isomerization of **3** to **4** (Table IV) were sealed in NMR tubes and immersed in an oil bath at 61 ± 1 °C. They were periodically withdrawn, and the extent of the isomerization was monitored by ^{19}F NMR spectroscopy. A quantitative material balance by elemental analysis of the 100% recovered cis and trans isomers established that only **3** and **4** were present at the end of the reaction. Rate constants and their standard deviations, calculated by using standard methods,[23] appear in Table IV.

Crystal Growth. Repeated recrystallization of **4** and **5** by the slow evaporation of their saturated solutions in CH_2Cl_2 gave crystals used for an X-ray crystallographic structure determination.

Crystal data for 4: $C_{18}H_{20}F_2O_2Te$, mol wt 434.0; monoclinic; a = 12.170 (3) Å, b = 11.976 (3) Å, c = 25.596 (5) Å, β = 111.26 (2)°, V = 3477 (1) Å^3, $F(000)$ = 1712 e, μ(Mo Kα) = 17.38. Systematic absences for hkl, $h + k = 2n + 1$, and for $h0l$, $l = 2n + 1$, established the space group as Cc or $C2/c$; successful refinement in the centrosymmetric space group confirmed $C2/c$ as the correct choice. The calculated density for Z = 8 was 1.658 g cm^{-3}, in good agreement with the experimental density of 1.67 g cm^{-3} measured by flotation in a mixture of methylene chloride and methylene bromide, and no symmetry was imposed on the molecule. A Syntex $P2_1$ diffractometer equipped with a graphite monochromator, λ(Mo K$\bar{\alpha}$) = 0.71069 Å, was used to obtain a data set and all parameters for a transparent distorted square-pyramidal crystal bound by faces ($0\bar{1}\bar{1}$), ($\bar{1}13$), ($00\bar{1}$), ($22\bar{3}$), and ($1\bar{1}2$). The perpendicular distance from the center of the crystal to each of the faces was 0.10, 0.10, 0.12, 0.20, and 0.22 mm, respectively. The quadrant $\pm hkl$ for $h + k = 2n$ was collected in the 2θ–θ scan mode for $3 \le 2\theta \le 50°$ with a variable scan rate between 2 and 29.3° min^{-1}. Each peak was scanned from 0.80° 2θ below the calculated Kα_1 peak position to 0.9° above the calculated Kα_2, and the background to scan time ratio was 0.25. Out of a total of 2871 unique reflections, 2577 were considered to be observed at the $3\sigma(I)$ criterion level. The data were corrected for Lorentz and polarization effects and numerically for absorption (maximum and minimum transmission factors were 0.705 and 0.575). The data were not corrected for secondary extinction.

Crystal data for 5: $C_{18}H_8F_{12}O_2Te$, mol wt 611.8; monoclinic; a = 9.154 (3) Å, b = 20.448 (6) Å, c = 10.829 (3) Å, β = 106.08(2), V = 1947.7(9) Å^3, $F(000)$ = 1168 e, μ(Mo Kα) = 16.52. Systematic absences for $h0l$, $l = 2n + 1$, and $0k0$, $k = 2n + 1$, establish the space group as $P2_1/c$. The calculated density for Z = 8 was 2.086 g cm^{-3} in good agreement with the experimental density of 2.08 g cm^{-3} measured by flotation in a mixture of methylene chloride and methylene bromide, and no symmetry was imposed on the molecule. A Syntex $P2_1$ diffractometer equipped with a graphite monochromator, λ(Mo K$\bar{\alpha}$) = 0.71069 Å, was used to obtain a data set and cell parameters for a transparent prismatic crystal bound by the following pairs of faces: (010), ($0\bar{1}0$), (012), ($0\bar{1}\bar{2}$), ($01\bar{1}$), ($0\bar{1}1$), (100), and ($\bar{1}00$); one damaged corner of the sample was estimated as the ($\bar{1}21$) face. The interfacial separations between the inversion related faces were 0.32, 0.36, 0.40, and 1.00 mm, respectively; the perpendicular distance from the center of the crystal to the ($\bar{1}21$) face was 0.4 mm. The quadrant $\pm hkl$ was collected in the 2θ–θ scan mode for $3 \le 2\theta < 55$ with a variable scan rate between 2.0 and 29.3 min^{-1}. Each peak was scanned from 0.9 2θ below the calculated Kα_1 peak position to 1.0° above the calculated Kα_2 and the background to scan time ratio was 0.25. Out of a total of 4467 unique reflections, 3873 were considered to be observed at the 3σ (I) criterion level. The data were corrected for Lorentz and polarization effects and numerically for absorption (maximum and minimum transmission factors were 0.621 and 0.552). The data were not corrected for secondary extinction.

Solution and Refinement. For both structures, coordinates for the tellurium atoms were deduced from a sharpened Patterson map. A weighted difference Fourier synthesis revealed positions for the remaining non-hydrogen atoms. Subsequent least-squares difference Fourier calculations gave positions for the hydrogen atoms in each case. In the final least-squares cycles, all non-hydrogen atomic positions were varied with anisotropic thermal coefficients and all hydrogen atom coordinates were varied with isotropic thermal parameters. The function minimized was $\sum w||F_o| - |F_c||^2$, where F_o and F_c are the observed and calculated structure factors, respectively. Refinement converged to conventional agreement factors of $R_1 = 0.026$ and $R_2 = 0.032$ ($R_1 = \sum||F_o| - |F_c||/\sum|F_o|$; $R_2 = |\sum w||F_o| - |F_c||^2/\sum w|F_o|^2|^{1/2}$) for **4** and $R_1 = 0.023$ and $R_2 = 0.030$ for **5**.

The final difference Fourier was featureless in both cases, and no systematic errors were apparent in the final observed and calculated structure factors. The positional parameters for **4** and **5** are shown in Tables I and II, respectively. The thermal parameters, structure factors, and a complete list of bond lengths and angles are available in supplementary material.

Results

Preparation of Telluranes. Telluranes **5**, **9**, and **10** were prepared by the method outlined in Scheme I. The low solubility

(23) Wentworth, W. E. *J. Chem. Educ.* **1965**, *42*, 96.

Table I. Final Coordinates of Pertellurane **4**[a]

atom	positional parameters		
	x/a	*y/b*	*z/c*
Te	0.23205 (1)	0.04528 (1)	0.14393 (1)
F	0.3345 (2)	0.0573 (2)	0.22214 (9)
F′	0.2687 (2)	−0.1125 (2)	0.15398 (9)
O	0.1448 (2)	0.0186 (2)	0.06495 (9)
O′	0.1965 (2)	0.2035 (2)	0.14369 (9)
C2	0.2057 (3)	0.0311 (3)	0.0269 (1)
C3	0.3336 (3)	0.0649 (2)	0.0598 (1)
C4	0.4144 (3)	0.0859 (3)	0.0340 (2)
C5	0.5271 (3)	0.1213 (3)	0.0663 (2)
C6	0.5610 (3)	0.1336 (3)	0.1236 (2)
C7	0.4836 (3)	0.1104 (3)	0.1501 (2)
C8	0.3707 (3)	0.0776 (2)	0.1169 (1)
C9	0.1418 (4)	0.1220 (6)	−0.0143 (2)
C10	0.1980 (5)	−0.0819 (5)	−0.0022 (3)
C2′	0.0940 (3)	0.2332 (2)	0.1564 (1)
C3′	0.0317 (3)	0.1277 (2)	0.1642 (1)
C4′	−0.0743 (3)	0.1278 (3)	0.1737 (2)
C5′	−0.1247 (3)	0.0297 (3)	0.1803 (2)
C6′	−0.0745 (3)	−0.0717 (3)	0.1772 (2)
C7′	−0.0306 (3)	−0.0753 (3)	0.1685 (2)
C8′	0.0807 (3)	0.0249 (2)	0.1622 (1)
C9′	0.1359 (5)	0.3020 (4)	0.2102 (2)
C10′	0.0145 (4)	0.3021 (4)	0.1068 (2)
H4	0.390 (6)	0.101 (6)	−0.011 (3)
H5	0.579 (3)	0.141 (3)	0.046 (1)
H6	0.638 (4)	0.151 (3)	0.145 (2)
H7	0.500 (3)	0.117 (3)	0.188 (2)
H8	0.058 (4)	0.102 (3)	−0.034 (2)
H9	0.148 (5)	0.176 (4)	0.002 (2)
H10	0.169 (4)	0.127 (4)	−0.045 (2)
H11	0.236 (3)	−0.136 (3)	0.029 (2)
H12	0.115 (4)	−0.104 (4)	−0.020 (2)
H13	0.242 (5)	−0.082 (5)	−0.025 (2)
H4′	−0.101 (3)	0.186 (3)	0.177 (1)
H5′	−0.190 (4)	0.031 (3)	0.190 (2)
H6′	−0.113 (3)	−0.131 (3)	0.182 (1)
H7′	0.065 (3)	−0.137 (3)	0.169 (2)
H8′	0.199 (4)	0.260 (4)	0.238 (2)
H9′	0.172 (4)	0.369 (4)	0.200 (2)
H10′	0.073 (3)	0.335 (3)	0.221 (2)
H11′	−0.046 (4)	0.334 (4)	0.107 (2)
H12′	0.001 (4)	0.267 (4)	0.078 (2)
H13′	0.072 (4)	0.363 (4)	0.106 (2)

[a] Estimated standard deviation in parentheses.

Scheme I

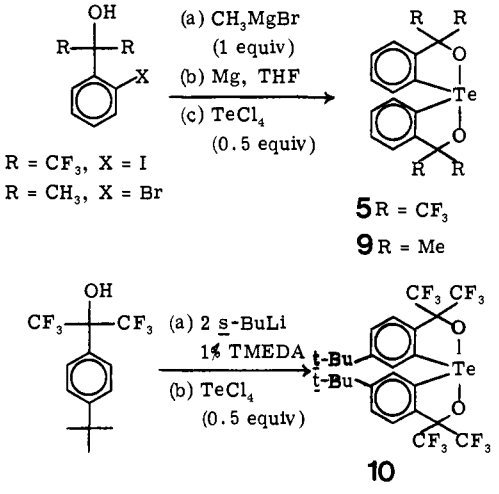

of **5** is increased in **10** by the presence of a *tert*-butyl substituent to the phenyl ring.

Structures of 4 and 5. Figures 2 and 3 show the stereoviews of a single molecule and the packing in the unit cell of pertellurane **4**, obtained by an X-ray crystallographic structure determination. Figures 4 and 5 show comparable views of tellurane **5**. Selected

Table II. Final Coordinates of Tellurane **5**[a]

atom	positional parameters		
	x/a	*y/b*	*z/c*
Te	0.25610 (2)	0.04026 (1)	0.01863 (1)
F1	0.6602 (2)	0.03212 (9)	0.4525 (2)
F2	0.5241 (2)	−0.03618 (9)	0.3216 (2)
F3	0.7346 (2)	−0.0038 (1)	0.2955 (2)
F4	0.5533 (2)	0.17874 (9)	0.1755 (2)
F5	0.6967 (2)	0.1516 (1)	0.3603 (2)
F6	0.7423 (2)	0.1154 (1)	0.1890 (2)
F1′	−0.1327 (2)	0.1429 (1)	−0.3666 (2)
F2′	−0.0247 (2)	0.0498 (1)	−0.3209 (2)
F3′	−0.2247 (2)	0.0718 (1)	−0.2654 (2)
F4′	0.0141 (2)	0.2023 (1)	0.0123 (2)
F5′	−0.1358 (2)	0.2226 (1)	−0.1733 (2)
F6′	−0.1940 (2)	0.1496 (1)	−0.0545 (2)
O	0.4857 (2)	0.04482 (9)	0.1164 (2)
O′	0.0318 (2)	0.06905 (9)	−0.0626 (2)
C2	0.5259 (3)	0.0705 (1)	0.2405 (2)
C3	0.3873 (3)	0.0908 (1)l	0.2826 (2)
C4	0.3928 (3)	0.1163 (2)	0.4031 (3)
C5	0.2597 (4)	0.1303 (2)	0.4330 (3)
C6	0.1202 (3)	0.1200 (2)	0.3456 (3)
C7	0.1122 (3)	0.0953 (2)	0.2243 (3)
C8	0.2469 (3)	0.0821 (1)	0.1941 (2)
C9	0.6132 (3)	0.0147 (2)	0.3292 (3)
C10	0.6314 (3)	0.1297 (2)	0.2422 (3)
C2′	0.0054 (3)	0.1220 (1)	−0.1460 (2)
C3′	0.1530 (3)	0.1503 (1)	−0.1623 (2)
C4′	0.1608 (3)	0.2029 (1)	−0.2413 (3)
C5′	0.2996 (3)	0.2242 (2)	−0.2516 (3)
C6′	0.4327 (3)	0.1924 (2)	−0.1857 (3)
C7′	0.4266 (3)	0.1401 (1)	−0.1064 (3)
C8′	0.2870 (3)	0.1202 (1)	−0.0937 (2)
C9′	−0.0949 (3)	0.0961 (2)	−0.2776 (3)
C10′	−0.0794 (3)	0.1748 (2)	−0.0905 (3)
H4	0.481 (3)	0.123 (1)	0.460 (3)
H5	0.266 (3)	0.145 (2)	0.513 (3)
H6	0.026 (3)	0.129 (2)	0.371 (3)
H7	0.014 (3)	0.084 (2)	0.165 (3)
H4′	0.078 (3)	0.223 (1)	−0.282 (3)
H5′	0.310 (3)	0.255 (1)	−0.301 (3)
H6′	0.534 (3)	0.213 (1)	−0.191 (3)
H7′	0.514 (3)	0.118 (1)	−0.058 (2)

[a] Estimated standard deviation in parentheses.

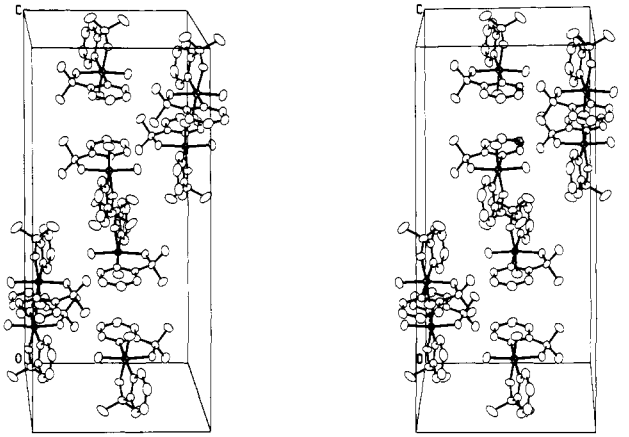

Figure 3. Stereoscopic view of the crystal structure of **4**. Hydrogen atoms have been omitted for clarity.

bond lengths and angles of **4**, **5**, and sulfurane **6**[18] are given in Table III.

An unusual feature of the structure of tellurane **5** is the lack of close intermolecular contacts between tellurium and nucleophilic sites in adjacent molecules. The crystal structures of the 10-Te-4 species TeX_4 (X = F, Cl, Br, I),[24] $(p\text{-}ClC_6H_4)_2$ TeI_2,[25a]

(24) (a) Engelbrecht, A.; Sladky, F. *Int. Rev. Sci.: Inorg. Chem. Ser. Two*, **1975**, *3*, 137. (b) Paulat, V.; Krebs, B. *Angew. Chem.* **1976**, *88*, 28. (c) Buss, B.; Krebs, B. *Ibid.* **1970**, *82*, 446.

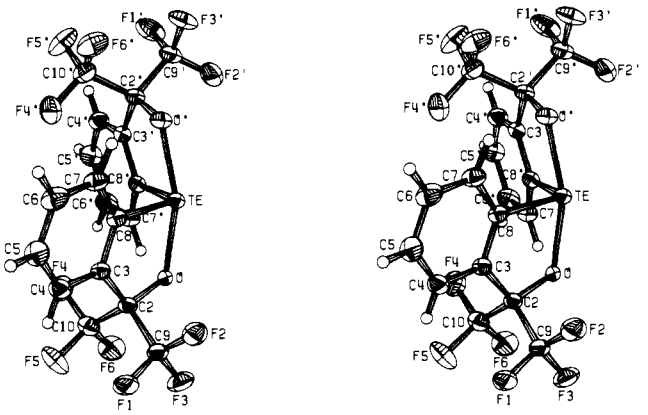

Figure 4. Stereoscopic view of a single molecule of tellurane **5**.

Ph_2TeBr_2,[25b] and **11** show much shorter intermolecular contacts with bridging atoms making the tellurium atoms resemble octahedral species. Closer approach of the nucleophilic oxygen atoms to the tellurium atom of a neighboring molecule is blocked by the bulky CF_3 groups. The intermolecular Te–O distances (3.559 (2) Å and 3.586 (2) Å) are very close to the sum of the van der Waals' radii for Te and O of 3.6 Å.[26] The shortest intermolecular Te–F_3 distance, 3.591 (2) Å, is also very close to the sum of the van der Waals' radii for Te and F of 3.55 Å.[26] There are no intermolecular contacts less than the sum of the van der Waals' radii of the atoms of **2**,[15] **4**, or **6**.[18]

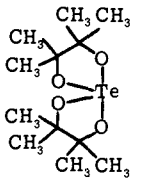

11

If the tellurium atom of **5** is placed at the origin of an orthogonal coordinate system in which the z axis is parallel to a line joining the two oxygen atoms, the Te–O and Te–O′ bonds are each displaced 9.8° from the yz plane, while the Te–C_8′ bond is displaced 5° above the xy plane and the Te–C_8 bond is 5° below the xy plane.

Reaction of 5 and 9 with Ozone. Trifluoromethylated tellurane **5** is inert toward ozone between −80 °C and 25 °C in CH_2Cl_2, while **9** undergoes facile oxidation to tellurane oxide dimer **12**. The mass spectrum of **12** shows a molecular ion at m/e 828 as well as peaks for $M^{+\cdot} - CH_3$ at m/e 813, and a large peak (71% relative intensity) for the monomeric tellurane oxide. Vapor-phase osmometry at 25 °C gave an experimental molecular weight of 820 (theoretical, 824) for dimer **12**. This makes it unlikely that there is any appreciable dissociation in solution at the concentrations used (ca. 10^{-2} M), or any significant association to give higher polymers. Compound **12** has two diastereomeric forms, each of which has two nonequivalent methyl groups. A 360-MHz ^1H NMr spectrum of **12** shows two large singlets for methyl protons at 1.40 and 1.71 ppm, and two small singlets for methyl protons at 1.45 and 1.57 ppm. The two large singlets comprise 88% of the area of the total for the four methyl singlets. It is possible that steric interactions between the bulky methyl groups in the achiral stereoisomer, **12a**, are sufficient to cause the predominance of the less hindered chiral diastereomer, **12b**. The two stereoisomers were not resolved by thin-layer chromatography. Alternative structures **12c** and **12d** are also compatible with the NMR spectra of these products. In view of the thermodynamic preference, established in this research, for pertellurane stereoisomers **2** and **4**, with trans aryl ligands and cis oxygen-centered ligands, there may be some basis for preferring structures **12c** and **12d**.

Table III. Selected Bond Lengths and Angles for Pertellurane **4**,[a] Tellurane **5**, Sulfurane **6**,[b] and Persulfurane **2**[a]

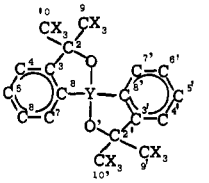

2, 4, 5, 6

	4, Y = TeF_2; X = F	**2**, Y = SF_2; X = F	**6**, Y = S; X = F	**5**, Y = Te; X = F
	Bond Lengths (Å)			
Y–F	1.942 (2)	1.627 (3)		
Y–F′	1.937 (2)			
Y–O	1.939 (2)	1.717 (2)	1.832 (5)	2.077 (2)
Y–O′	1.943		1.819 (5)	2.082 (2)
Y–C	2.078 (3)	1.804 (3)	1.787 (8)	2.106 (2)
Y–C′	2.073 (3)		1.803 (8)	2.103 (2)
	Bond Angles (deg)			
F–Y–F′	84.50 (9)	86.48 (9)		
O–Y–O′	96.91 (9)	93.9 (1)	177.1 (2)	160.53 (7)
C–Y–C′	172.7 (1)	173.3 (1)	108.1 (4)	104.58 (10)
F–Y–O	172.28 (9)	89.84 (9)		
F–Y–O′	89.45 (9)	175.74 (9)		
F–Y–C	91.9 (1)	90.7 (1)		
F–Y–C′	93.9 (1)	92.7 (1)		
F′–Y–O	89.45 (9)			
F′–Y–O′	172.71 (9)			
F′–Y–C	93.9 (1)			
F′–Y–C′	92.1 (1)			
O–Y–C	83.6 (1)	89.5 (1)	85.8 (3)	79.01 (8)
O–Y–C′	91.1 (1)	87.3 (1)	91.3 (3)	88.89 (8)
O′–Y–C	91.4 (1)		92.2 (3)	89.16 (8)
O′–Y–C′	84.3 (1)		87.1 (3)	79.10 (8)
Y–C_8′–C_3′	109.6 (2)		112.8 (3)	114.4 (2)
C_8′–C_3′–C_2′	119.6 (3)		113.6 (4)	116.8 (2)
C_3′–C_2′–O′	109.7 (2)		108.5 (6)	111.8 (2)
C_2′–O–Y	116.7 (2)		114.4 (4)	118.0 (1)
Y–C_8–C_3	109.9 (2)	112.6 (2)	114.8 (5)	114.5 (2)
C_8–C_3–C_2	119.5 (3)	112.9 (3)	112.3 (5)	116.7 (2)
C_2–C_2–O	109.0 (2)	107.8 (2)	107.5 (4)	111.9 (2)
C_2–O–Y	117.9 (1)	116.9 (2)	114.2 (4)	117.9 (1)

[a] Estimated standard deviation in parentheses. [b] Reference 18. [c] Reference 15.

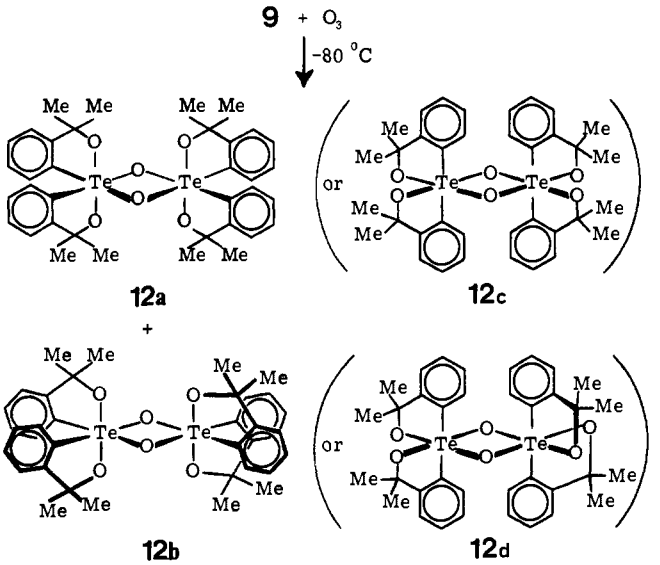

Equilibration between the two diastereomers is not observed up to 100 °C. Decomposition of the dimer occurs above 100 °C in chlorobenzene solution to give unidentified products.

(25) (a) Chao, G. Y.; McCullough, J. D. *Acta Crystallogr.* **1962**, *15*, 887. (b) Christofferson, G. D.; McCullough, J. D. *Ibid.* **1958**, *11*, 249.

(26) Pauling, L. "The Nature of the Chemical Bond", 3rd ed.; Cornell University Press: Ithaca, NY, 1960; p 260.

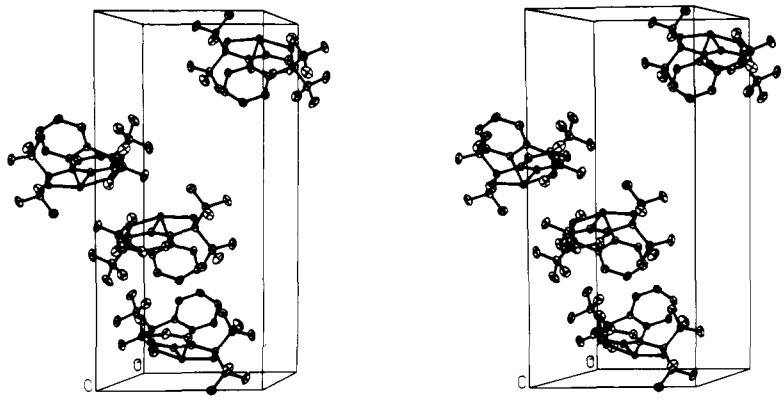

Figure 5. Stereoscopic view of the crystal structure of **5**. Hydrogen atoms have been omitted for clarity.

Stereochemistry of Pertelluranes 3, 4, and 13. The ^1H and ^{19}F NMR spectra of **3** show a singlet for the methyl protons at 1.71 ppm and a singlet for the fluorines attached to tellurium at −25.9 ppm. The ^1H and ^{19}F NMR spectra of **13** show a singlet for the methyl protons at 1.46 ppm, a singlet for the fluorine atoms attached to tellurium at −63.4 ppm, and a singlet for the CF_3 fluorines at −75.7 ppm, consistent with either (*OC*-6-12)[16] isomers **3, 13**, or (*OC*-6-13) stereoisomers **14** and **15**. We prefer (*OC*-6-12) structures **3** and **12** by analogy with the kinetically preferred formation of (*OC*-6-12)-*trans*-persulfurane **1** under the same experimental conditions.[15]

Pertellurane **3**-(*OC*-6-12)[16] isomerizes rapidly at room temperature, in the presence of catalytic amounts of the Lewis acid sulfur trioxide, to give the more stable cis isomers **4**-(*OC*-6-22). The ^{19}F and ^1H NMR spectra of **4** show a singlet for the fluorine atoms of **4** at −51.6 ppm and a doublet for the nonequivalent methyl protons at 1.55 and 1.62 ppm. The NMR spectra do not rule out structure **16**-(*OC*-6-33) as an alternative for **4**. An X-ray crystallographic structure determination was necessary to show **4** to be the proper structure.

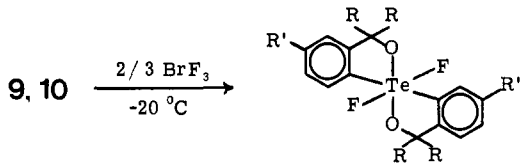

3 R = Me, R' = H
13 R = CF_3, R' = t-butyl

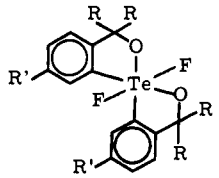

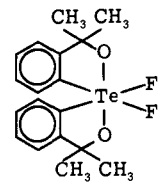

14 R = CH_3, R' = H
15 R = CF_3, R' = t-butyl

16

In quinoline solution, a basic medium lacking a strong Lewis acid necessary for catalysis of the dissociative process, the isomerization of **3** to **4** requires heating at 60 °C for about 60 h to reach the equilibrium ratio of **4** to **3** (approximately 9:1). In order to gain evidence for the mechanism of the isomerization of **3** to **4** at higher temperature in the absence of Lewis acid, we carried out the rate measurements reported in Table IV. Reactions were followed by ^{19}F NMR spectroscopy. At temperatures above 100 °C, in quinoline or diphenyl ether, difluoropertellurane **3** is reduced to tellurane **9**. Aromatic fluorination products, observed by ^{19}F NMR, were not identified.

The isomerization of pertellurane **13** in the presence of Lewis acids does not occur under conditions at which **3** is rapidly converted to **4**. It was unaffected by heating at 60 °C for 3 days with 0.075 M SbF_5. Nor was the thermal isomerization of molten **13** observed upon heating it to 210 °C at 0.4 torr for 4 days. This sets a lower limit of 44 kcal/mol for the activation barrier for the thermal isomerization of **13** at this temperature in the absence of Lewis acids.

Table IV. Rate Constants for the Isomerization[a] of **3** to **4** at 61 °C

solvent[b]	10^2[**1**] initial, M	no. of half-lives followed	10^5k_1, s^{-1}	Y[f]
CH_2Cl_2	5.9	3	2.40 ± 0.05	−5.57
CH_2Cl_2	13.2	3	2.40 ± 0.05	
CH_2Cl_2[c]	6.7	3	2.51 ± 0.05	
$CH_2Cl/HN(SiMe_3)_2$[d]	5.1	3	2.0 ± 0.1	
benzene/toluene[e]	1.1	2	2.0 ± 0.2	−8.62

[a] A quantitative material balance established the presence of only **3** and **4** at the completion of each reaction. [b] The reactions were run in sealed NMR tubes. [c] With 0.03 M KF/18-crown-6. [d] In 80% CH_2Cl_2/20% $HN(SiMe_3)_2$, by weight. [e] In 50% benzene/50% toluene, by weight, with 0.5% by weight of added $HN(SiMe_3)_2$. [f] These Y values were used to calculate m according to the equation $\log k/k_0 = mY$. The Y values were calculated from measured Z values by using the equation $Y = 0.29887Z - 24.758$ on p 302 of ref 28.

Table V. ^{125}Tellurium Chemical Shifts and Coupling Constants for Selected Organotellurium Compounds

compd	^{125}Te NMR[a]	$^1J_{Te-F}$, Hz
3	985	2108
4	1066	2629
5	1196	
9	1051	
10	1190	
13	1007	2815

[a] Chemical shifts are measured in ppm downfield from Me_2Te.

The ^{125}Te NMR chemical shifts of the tellurium atoms of new compounds of this paper are listed in Table V. The magnitude of the Te–F coupling constants for 12-Te-6 compounds **3**, **4**, and **13** are lower than that reported[22a] for TeF_6 (3688 Hz) and F_5-TeOCl (3755 Hz). The ^{125}Te chemical shifts of **3**, **4**, **5**, **9**, **10**, and **13** fall within the range of those reported[22b] for other 10-Te-4 and 12-Te-6 species.

Discussion

Mechanism of Formation of Pertelluranes 3 and 12 and the Acid-Catalyzed Isomerization of 3 to 4. The fluorinations of telluranes **9** and **10** with bromine trifluoride probably proceed through the unobserved 10-Te-5 pertelluronium cations (**17** and **18**) by a mechanism similar to that proposed[15] for the formation of **1**. We have earlier discussed[15] frontier orbital considerations favoring attack of fluoride ion (or a fluoride ion equivalent) at the σ^* orbital of the S–F bond of a closely related 10-S-5 persulfonium ion to give the *OC* product in which the two fluorine ligands are trans. Similar arguments may be advanced for the formation of tellurium species **3** and **13** from **9** and **10**.

The acid-catalyzed isomerization of *all-trans*-(*OC*-6-12)[16]-persulfurane **1** to *cis*-(*OC*-6-22)-persulfurane **2** was postulated to proceed by dissociation to give a 10-S-5 persulfonium cation.

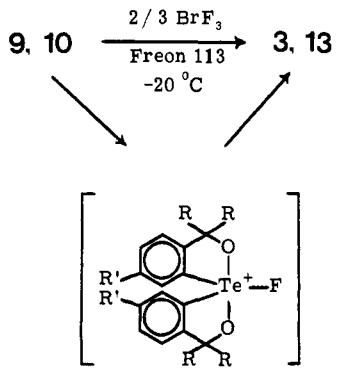

17 R = CH_3, R' = H
18 R = CF_3, R' = t-butyl

This cation was subsequently isolated and characterized as a hexafluorophosphate salt of the cation.[15] It is reasonable to postulate a similar mechanism for the acid-catalyzed isomerization of **3** to **4**. Acid-catalyzed ionization of **3** could generate 10-Te-5 pertelluronium ions **17** (path a) or **19** (path b), species interconvertible by a single pseudorotation step. The higher energy[15] isomer, **19**, could recombine with fluoride in the equatorial plane either to regenerate **3** or to form the thermodynamically more stable **4**. Fluoride attack in the equatorial plane of **17** could provide either **3** or the never observed (*OC*-6-22) isomer, **16**.

Addition of **3** to solutions of antimony pentafluoride, under conditions which give the persulfonium ion from **1**,[15] results in an equilibrium mixture of **3** and **4** by acid-catalyzed isomerization of **3**. Although the lower electronegativity of tellurium compared to sulfur might lead one to predict that the tellurium atom of a 10-Te-5 pertelluronium cation could more easily accommodate a positive charge than the sulfur of a 10-S-5 persulfonium cation, the 10-Te-5 species is not observed. A pentacoordinate 10-Te-5 tellurane oxide has been suggested as an intermediate in, e.g., the reaction of an alkyltrichlorotellurane with *tert*-butyl hydroperoxide,[29] but no direct evidence has been reported for andy 10-Te-5 structures in solution.[30] At high temperature $B(OTeF_5)_3$[31] and $LiOTeF_5$[32] give the dimer of the expected tellurane oxide, F_4TeO, plus polymers.

While the bidentate ligands of compounds **5**, **9**, and **10** (with electronegative apical substituents and electropositive equatorial substituents) are designed to stabilize the TBP geometry,[33] we have not observed pentacoordinate 10-Te-5 species which incorporate these bidentate ligands. The oxidation of tellurane **9** gives only dimer **12**, without amounts of monomer detectable by ^1H NMR or osmometry in ca. 0.02 M solutions. The large size of the tellurium atom relative to that of sulfur sterically favors larger coordination numbers[30] for tellurium than for sulfur, consistent with our failure to observe a 10-Te-5 pertelluronium species from solutions of **3** and antimony pentafluoride. Despite the fact that the ligands of **3** are less electron withdrawing than those of **1**, a 10-S-5 persulfonium ion is formed from **1** under these conditions.[15]

Thermal Isomerization of Pertellurane 3 to 4. In marked contrast to persulfurane **1**, which is unaffected[15] by prolonged heating at 238 °C in quinoline, tetramethyl-*trans*-pertellurane **3** is almost completely converted to **4**, its cis isomer, after 3 days in quinoline at 60 °C. This suggests that the uncatalyzed ligand rearrangement about tellurium proceeds readily by a nondissociative route. In order to test this postulate, we carried out the kinetic studies reported in Table IV.

Scheme II

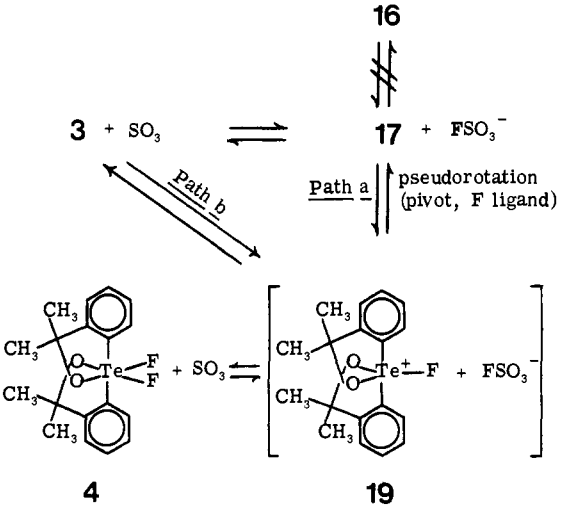

4 **19**

Doubling the concentration of **3** does not affect the first-order isomerization rate constants, nor does the addition of fluoride ion. These observations rule out (inter alia) an associative isomerization mechanism involving attack of fluoride at tellurium to form a heptacoordinate intermediate or transition state.

Dissociative mechanisms are difficult to rule out for complexes with one or more bidentate ligands. Heterolysis of a Te–O bond of **3** would give a five-coordinate zwitterionic intermediate which could rearrange before reforming the Te–O bond to give **4**. Although intramolecular, such a process is dissociative. Heterolysis of a Te–F bond to give an ion pair could similarly result in rearrangement of the TBP cation within the ion pair. Reforming the Te–F bond, if faster than dissociation of the ion pair, could therefore provide a route for isomerization which is also clearly intramolecular, though dissociative. The failure to trap fluoride ion during the rearrangement of **3** in media containing hexamethyldisilazane[34] provides strong evidence against the intermediacy of dissociated fluoride ion, but it does not rule out the intermediacy of fluoride ion in an intimate ion pair.

The ion-pair mechanism (Te–F heterolysis) and the zwitterion mechanism (Te–O heterolysis) are both ruled out by the observation that the rate of isomerization is very insensitive to solvent ionizing power, decreasing only ca. 20% on changing from CH_2Cl_2 to the less polar benzene/toluene as a solvent. The value of m in the Grunwald–Winstein equation[28,35] ($\log k/k_0 = mY$) is a measure of the sensitivity of the reaction system being studied to changes in solvent ionizing power. The quantity Y is a measure of the ionizing power of the solvent. The data of Table IV gives an m value of 0.03 for the rearrangement of **3**. Representative m values for other reactions which one would expect to proceed with rates relatively insensitive to changes in solvent ionizing power, for example, the Diels–Alder dimerization of cyclopentadiene,[36] or the addition of fumaronitrile to 9,10-dimethylanthracene,[37] are comparable in value (0.02 and 0.07, respectively). A heterolytic reaction which proceeds via a transition state resembling an ion pair, for example, the ionization of *p*-methoxyneophyl tosylate,[38] gives a value for m of 0.50 ± 0.08.[39] The rate change expected for such an ionization in solvents with differences in ionizing power comparable to the range used in the experiments of Table IV is

(27) Day, R. O.; Holmes, R. R. *Inorg. Chem.* **1981**, *20*, 3071.
(28) Kosower, E. M. "An Introduction to Physical Organic Chemistry"; Wiley and Sons: New York, 1968.
(29) Uemura, S.; Fukuzawa, S. *J. Chem. Soc., Chem. Commun.* **1980**, 1033.
(30) Seppelt, K. *Angew. Chem., Int. Ed. Engl.* **1979**, *18*, 186.
(31) Sladky, R.; Kropshofer, H.; Lietzke, O. *J. Chem. Soc., Chem. Commun.* **1973**, 134.
(32) Seppelt, K. *Z. Anorg. Allg. Chem.* **1974**, *406*, 287.
(33) Perozzi, E. F.; Michalak, R. S.; Figuly, G. D.; Stevenson, W. H., III; Dess, D. B.; Ross, M. R.; Martin, J. C. *J. Org. Chem.* **1981**, *46*, 1049.
(34) Ibbott, D. G.; Janzen, A. F. *Can. J. Chem.* **1972**, *50*, 2428.
(35) Lowry, T. H.; Richardson, K. S. "Mechanism and Theory in Organic Chemistry", 2nd ed.; Harper and Row: New York, 1981; p 328.
(36) Cöster, G.; Pfeil, E. *Chem. Ber.* **1968**, *101*, 4248.
(37) (a) Sauer, J.; Wiest, H.; Mielert, A. *Chem. Ber.* **1964**, *97*, 318. (b) Sauer, J. *Angew. Chem., Int. Ed. Engl.* **1967**, *6*, 16.
(38) Smith, S. G.; Fainberg, A. H.; Winstein, S. *J. Am. Chem. Soc.* **1961**, *83*, 618. The Dimroth E_T values[28] for $ClCH_2CH_2Cl$, CH_2Cl_2, benzene, and toluene are 41.9, 41.1, 34.5, and 33.9, respectively. The solvents used in the kinetic studies of the ionization of *p*-methoxyneophyl tosylates included pyridine, acetone, and diethyl ether, which have very similar E_T values of 40.2, 42.2, and 34.6, respectively.
(39) For a list of m values for other systems, see p 336 of ref 35.

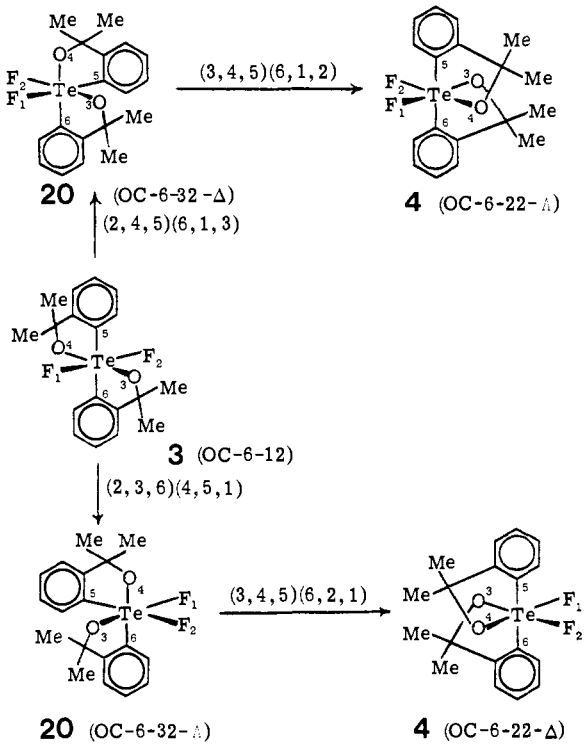

Figure 6. Proposed nondissociative pathway for the isomerization of **3** to **4**. The designation (a, b, c) (d, e, f) refers to the process in which substituents a, b, and c are eclipsed by d, e, and f, respectively, in the trigonal prismatic transition state of a C_3 twist. See ref 7d for a discussion of the fact that alternative C_2 and C_3 formulations of twist mechanisms give identical products. They are properly viewed as minor variations of the same mechanism (ref 7b). The designation of stereochemistry, enclosed in parentheses following the number of the compound, employs the formalism of Brown, Cook, and Sloan.[16]

greater than two orders of magnitude. The small (ca. 20%) rate increase observed for the isomerization of **3** on going from benzene/toluene to methylene chloride as solvent is of the magnitude expected for the development of a small dipole moment in the transition state for the isomerization. While **3** can have no dipole moment, **4** is expected to have one, as is the transition state separating the two, even in the absence of bond heterolysis.

These results provide strong evidence for a mechanism which involves neither dissociation nor association, a nondissociative intramolecular ligand permutation about the central tellurium atom. The isomerization of **3** to **4** by one of the proposed idealized twist processes[9-11] proceeds by way of an intermediate ψ-OC geometry (**20**), in which all the pairs of equivalent C, F, and O substituents are cis [(*OC*-6-32),[16] Figure 6]. We have, however, no direct evidence for the intermediacy of **20**; it may be an energy maximum rather than minimum. If this mechanism is operative with **20** as an intermediate, rather than a transition state, **20** must be relatively high in energy and quickly converted to **4**.

Substituent Effects on the Rates of Isomerization of 12-Te-6 Species. The CF_3-substituted pertellurane (**3**) does not isomerize either under the conditions of acid catalysis effective for persulfurane **1**[15] or upon heating in the absence of Lewis acids. If this failure to react is kinetic in origin the lower limit for the free energy of activation for a nondissociative rearrangement of **13** is 44 kcal/mol, at least 17 kcal/mol greater than that (27 kcal/mol) for the thermal rearrangement of **3** in quinoline. In the absence of any other evidence this would suggest the operation of a dissociative mechanism for the isomerization of **3** in the absence of Lewis acids. The Te–F bond heterolysis to give the cationic pertelluronium ion is expected to be slower for the species containing the more electron-withdrawing CF_3 substituents (see Scheme II).

Since we see no evidence for an isomer of **13** we must also consider the possibility that the failure of **13** to isomerize simply reflects the fact that it is the most stable of its set of stereoisomers.

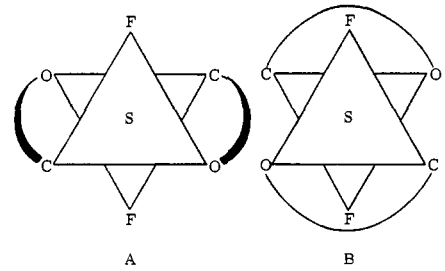

Figure 7. Projections of *trans*-(*OC*-6-12)-persulfurane **1** along two approximate threefold axes. All cis X–S–X angles are 90 ± 1°, corresponding closely to the twist angle of 60° characteristic of octahedral geometry.

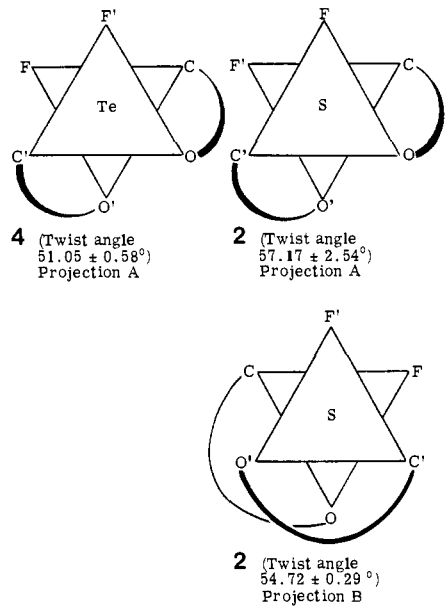

Figure 8. Twist angles of **2** and **4**. These angles were calculated for projection A by projecting the atoms on a plane which contains the midpoint of the F–F′ vector, the bisector of the angle formed by the F–S–C (or F–Te–C) bisector, and the central atom. For projection B the plane contains the midpoint of the F–F′ vector, the bisector of the angle formed by the F′–S–C bisector and the C–S–O′ bisector, and the central atom. Twist angles for each projection are calculated as the mean of the deviations of the projected interfacial twist angles from the ideal 60°, with the sign of the deviation taken in the sense determined from the direction of the twist angle from 60° (larger or smaller) recognizing that the ideal trigonal twist deforms adjacent interfacial angles in the projection in the opposite senses, increasing one angle while decreasing the adjacent angle. The standard deviation of the twist angle is therefore a measure of the regularity of the trigonal twist about the axis of the projection.

The difference in energy between the *all-trans*-(*OC*-6-12) stereoisomers **1** and **3** and the more stable *cis*-(*OC*-6-22)[16] isomers **2** and **4** to which they rearrange (1.6 and 1.4 kcal/mol, respectively) is so small and the reasons for the order of stabilities are so poorly understood[15] that we cannot rule out the possibility that the order of stabilities is reversed for CF_3-substituted pertellurane **13**.

Hofmann, Howell, and Rossi have pointed out[12] that the energetic preference for *OC* geometry relative to *TP* geometry for hexacoordinate 12-S-6 sulfur species stems primarily from two causes: (a) ligand–ligand repulsive interactions are greater in the *TP* than in the *OC* geometry; (b) there is also a pronounced increase in energy of the two filled e_g orbitals of the *OC* species as they are transformed into the higher energy e″ orbitals of the *TP* geometry. In the absence of d-orbital interaction these orbitals are entirely localized on the ligands. They are, however, of proper symmetry to interact with empty d orbitals on the central atom. Since d orbitals are higher in energy than the ligand orbitals, the importance of this interaction is greater with the filled e″ orbitals of the *TP* transition state for a twist mechanism than with the

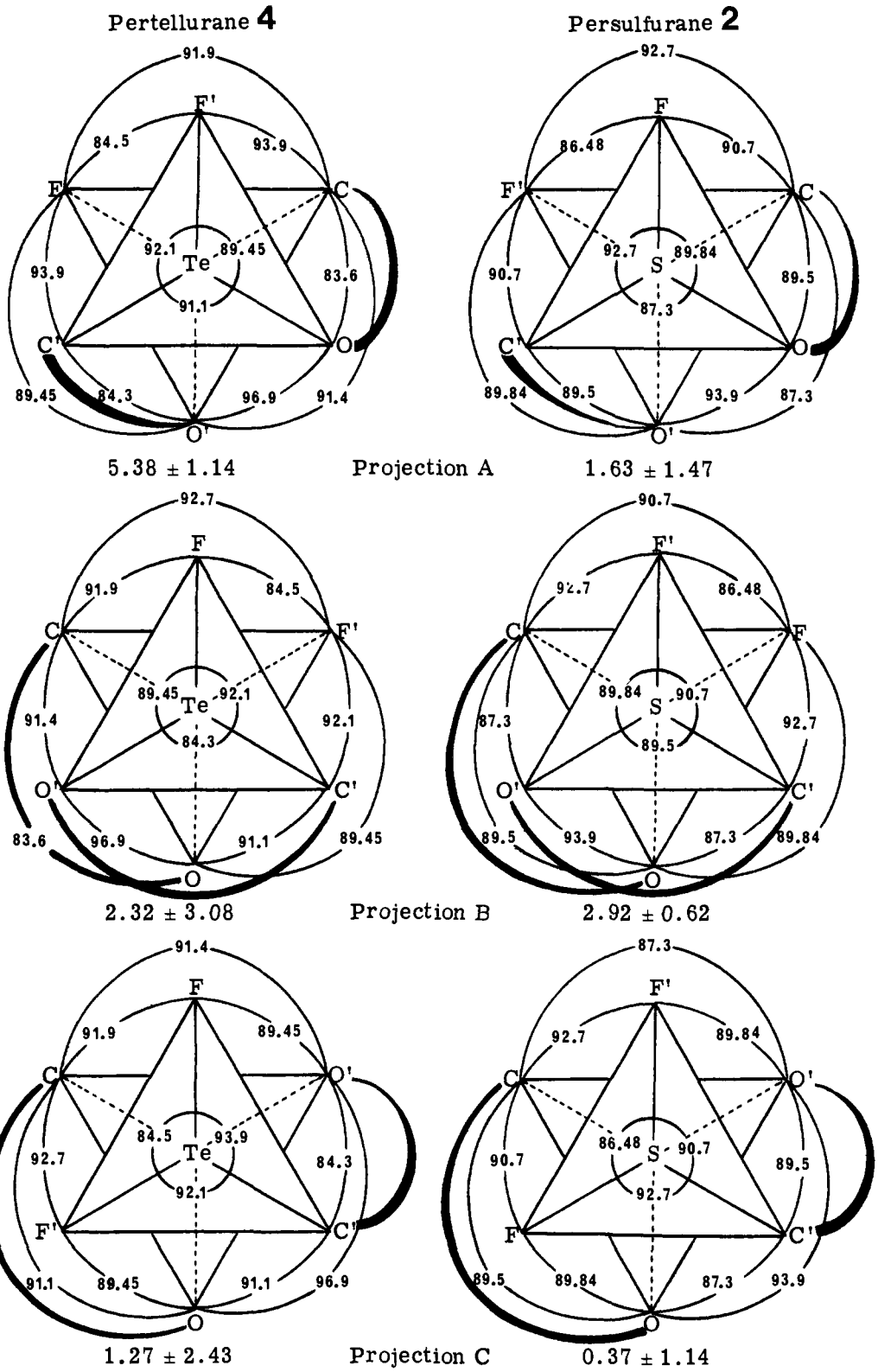

Figure 9. Actual bond angles (in degrees) of **2** and **4** recorded on projections along their approximate threefold axes. The average deviations of the interfacial bond angles from 90° (the quantities printed under each projection) were calculated as the mean of the deviations of the interfacial bond angles from the ideal 90°, with the sign of the deviation taken in the sense determined from the direction of the deviation from 90° (larger or smaller) recognizing that the ideal trigonal twist deforms adjacent interfacial angles in the projection in opposite senses, increasing one angle while decreasing the adjacent angle. The standard deviation of the average deviation is therefore a measure of the amount of distortion from *OC* geometry in a projection.

e_g orbitals of the *OC* ground state, because the e″ orbitals are closer in energy to the empty d orbitals. The calculated difference in energy is therefore less when d orbitals are included in the calculation.

We can extend this argument to explain the greater stereolability of **3** compared to **13**. The lowering in energy of the e″ ligand orbitals which accompanies the replacement of the CH_3 groups of **3** with the more electronegative CF_3 groups of **13** decreases the importance of d-orbital interactions in the CF_3 case (**13**). This effect would therefore contribute to an increased activation barrier for the twist isomerization of **13**, where this d-orbital stabilization is less important, than for **3**, where increased d-orbital participation

is expected. This provides one rationalization of our observations, if indeed the failure to observe an isomerization of **13**-(*OC*-6-12)[16] to its *OC*-6-22 isomer, parallel to that observed for **3**, does result from a high activation barrier for the process interconverting the two, rather than a reversal in the order of ground-state energies.

The Geometry of the Five-Membered Ring in Telluranes and Pertelluranes. The geometry about the central tellurium atom of tellurane **5** is *ψ-TBP* with an angle of 160.53 (7)° between the apical bonds. The comparable bond angle in the isostructural periodonium cation **7**[19] is 162.8°, and that for tetraoxytellurane **11**[27] is 153.5°. These apical bonds are all severely distorted (in the same direction—away from the lone pair of electrons) from the idealized *TBP* bond angle of 180°. The distortion is in the direction predicted by electron pair repulsion theory.[40] It has been suggested[27] that the deformation in **11** is the result of intermolecular bonding interactions in the crystal lattice. Such an explanation seems unlikely for **5** or **7**[19b] in view of the long intermolecular contacts observed in their crystal structures. The apical bond deformations in compounds **5**, **7**, and **11** are the expected result of the strain induced in the five-membered ring by the longer bonds to the central atom (Table III). These longer bonds are accommodated in the five-membered ring of **5** by narrowing the endocyclic O–Te–C angle and opening the other endocyclic angles relative to those in sulfurane **6**. This accentuates the observed deformation in the O–Te–O angle resulting from bending the weak[41] apical Te–O bonds. Both Te–O and Te–C bonds are shorter in pertellurane **4** than in tellurane **5**, which makes the five-membered rings of **4** less strained than those of **5**. The structure of **4** does not therefore exhibit as large a distortion from idealized *OC* geometry as does **5** from *TBP* geometry.

Trigonal Distortion of the Octahedral Ground State of 12-X-6 Systems. Ground-state geometries intermediate between *OC* and *TP* may be described in terms of a twist angle, the angle between the triangles defined by the substituents on the upper and lower triangular faces of the octahedron, viewed down one of the threefold axes. The twist angle for an idealized *OC* geometry, 60°, decreases to 0° for an idealized *TP* geometry. An examination of distorted *OC* ground states can provide some insight into the probable course of the twist mechanism for the interconversion of *OC* isomers. Most hexacoordinate metal complexes that have been discussed in terms of *OC*–*TP* trigonal distortion have three bidentate ligands attached to the central atom. The observed *OC* → *TP* distortion is usually about the unique axis whose projection shows only interfacial bites[42] of the bidentate ligands with the direction of the twist toward the *TP* geometry with eclipsed bonding sites for each bidentate ligand. For many structures[43-45] the amount of trigonal distortion increases as the endocyclic bond angle at the metal, dictated by metal–ligand bond lengths, decreases.

Since *trans*-(*OC*-6-12)-persulfurane **1** has almost ideal *OC* geometry, with cis and trans bond angles of 90 ± 1° and 180 ± 1°, respectively, its twist angle is almost exactly the ideal 60° along each threefold axis. The relief of possible O–S–C angle strain in the five-membered rings of **1** by a trigonal distortion about the axis of projection A (Figure 7), with interfacial bites, is not possible since any twist distortion which decreases one O–S–C endocyclic bond angle must increase the other. A twist about the axis of projection B (Figure 7) could, however, result in a decrease in O–S–C bond angles if this would result in relief of angle strain. The lack of any appreciable distortion from *OC* geometry suggests that the five-membered rings of **1** are not the locus of appreciable angle strain in the *OC* geometry.

The narrowing of angles which must accompany a change from *OC* to *TP* geometry could be accommodated by distributing the angle deformation among the angles about the central atom in several different ways. If all angles were narrowed by equal amounts (i.e., intrafacial bond angles equal interfacial bond angles) in the TP transition state, the change in bond angles would be from 90° (*OC*) to 81° 48′ (*TP*).[11]

The distortion from *OC* geometry observed for *cis*-persulfurane **2** is greater than for *trans*-persulfurane **1**, but the endocyclic O–S–C angles are still within 0.5° of 90°. The longer bonds to tellurium in **4** introduce more ring strain which is relieved by a twist about the axis of projection A (Figures 8 and 9). The regularity of the twist deformation is obvious in the small uncertainty in the large (ca. 9°) twist deformation in projection A (Figure 8) from the 60° twist angle of a regular *OC* geometry, and in the regular alternation of observed interfacial[42] bond angles above and below the *OC* value of 90° from the perspective of projection A (Figure 9). This confirms the notion that most of the angle distortion for the *OC* → *TP* twist about a particular axis occurs in the interfacial angles. Projections B and C (Figure 9) show much less regular bond alternation. Most of the distortion of **4** from *OC* geometry has its origins in the narrowing of the bite of the bidentate ligands (the endocyclic interfacial angles of projection A). The F–Te–F angle, interfacial in projection A, is narrowed about as much as the endocyclic C–Te–O angles, even though monodentate ligands are involved.

The shorter bonds to the central atom of *cis*-persulfurane **2** result in its adopting a less distorted *OC* structure than that seen for the pertellurane. The deviations from 90° of interfacial bond angles of **2** in projections A and B (Figure 9) are much smaller than those for *cis*-pertellurane **4** and are much less regular. The small twisting about two different projections results in a larger standard deviation in the calculated average twist angle for **2** (Figure 8). Endocyclic angle strain is therefore not a major contributor to the distortion of **2**.

Conclusion

The greatly reduced activation barrier for the trigonal twist isomerization of 12-Te-6 species relative to analogous 12-S-6 species results, at least in part, from the effectiveness of the *OC*–*TP* distortion in relieving angle strain caused by the long bonds of bidentate rings to the central tellurium atom. If this structural feature, which lowers the activation barrier for the twist isomerization of **3** to **4** to 27 kcal/mol, is correctly credited with the stabilization of the *TP* transition state, it is reasonable to suggest that further lowering of the energy of activation by the further incorporation of such structural features should produce an octahedral nonmetal which might be fluxional at room temperature, like many *TBP* nonmetals.

Acknowledgment. This research was supported in part by a grant from the National Science Foundation (CHE 79-07-7905692). Mass spectra were obtained from facilities provided under grants from the National Institutes of Health (CA 11388 and GM 16864). The University of Illinois Midwest NSF Regional NMR Facility (CHE 79-16100) provided NMR spectra.

Registry No. 3, 92315-00-9; **4**, 92418-52-5; **5**, 92315-01-0; **9**, 92315-02-1; **10**, 92315-03-2; **12**, 92315-05-4; **13**, 92315-04-3; ^{125}Te, 14390-73-9.

Supplementary Material Available: A listing of the thermal parameters for **4** (Table VI) and **5** (Table VII), bond lengths and angles for **4** (Table VIII) and **5** (Table IX), and observed and calculated structure factor amplitudes for **4** (Table X) and **5** (Table XI) (34 pages). Ordering information is given on any current masthead page.

(40) Cotton, F. A. "Advanced Inorganic Chemistry", 4th ed; John Wiley and Sons: New York, 1980; p 206.

(41) (a) Kepert, D. L. *Inorg. Chem.* **1972**, *11*, 1561. (b) Reference 40, p 52.

(42) The term "intrafacial bite" refers to a projection in which a bidentate ligand spans two sites within a single triangular face, while the term "interfacial bite" refers to a bidentate ligand spanning sites on the two triangular faces of a projection of an *OC* molecule (see Figures 7, 8, and 9). A "small bite" is one which tends to narrow the endocylic angle at the *OC* atoms to a value less than 90°.

(43) Although most hexacoordinate transition-metal complexes show *OC* geometry several exhibit *TP* geometry, mostly species containing 1,2-dithiolene or 1,2-diselenolene ligands. An attractive "interligand donor atom bonding" force between adjacent atoms has been proposed[41b,44] for these compounds which would overcome electronic repulsions of the atoms. Such an attractive force is absent in **1**, **2**, and **4**.

(44) Schrauzer, G. N. *Acc. Chem. Res.* **1979**, *2*, 72.

(45) Avdeef, A.; Fackler, J. P., Jr. *Inorg. Chem.* **1975**, *14*, 2002.